Memo

To
Projectgroep slib VNSC

Date
27 June 2018

Number of pages
34

From
Miguel de Lucas Pardo
Bob Smits,
Yoeri Dijkstra

Direct line
+31(0)88335 7461

E-mail
miguel.delucaspardo@deltares.nl

Subject
Scheldt 2DV model_D3D-iflow hybrid approach

---

1 Introduction

Earlier work
This report builds up on the work presented in the 2016 Deltares report “Sediment transport in a schematized Scheldt. Regime Shift”. The goal of this previous report was to assess the conditions in which sediment was imported from the sea into the estuary, particularly to the water column, studying the transition to hyper-turbidity. A number of model configurations and sediment transport processes and parameters were evaluated to that end. The results showed that importing sediment to the water column was possible only for a certain period of time, reaching an equilibrium in the total amount of suspended sediments in the domain.

For some model configurations and/or sediment parameters, continuous accumulation of sediment in the bed was found. However, the eroding forces at these configurations were not large enough to bring the sediment into suspension, resulting in very small suspended sediment concentrations. For other model configurations and/or sediment parameters, most of the sediment in the bed was being eroded into the water column, resulting in higher suspended sediment concentrations. However, sediment did not accumulate in the model domain under these conditions, thus not arriving to equilibrium in the water column with depletion in the bed. Essentially, there were combinations of parameters that resulted in a turbid water column over an empty estuarine bed (with a net exporting effect over the entire estuary), and other parameter sets that resulted in relatively clean water columns over accreting river beds (with a net importing effect over the entire estuary). In an ideal situation sediment is brought into the water column while increasing the total sediment in the system. This situation was either non-existing or not found.

New work / outline of this memo
Rather than continuing testing new combinations of parameters and processes aiming for the ideal situation, the research team decided to go one step back and study if hyper-turbid conditions could ever be maintained in an estuary like the one in our study. Therefore, we stopped studying the dynamic process and focussed on the stationary process of hyper-turbid conditions. In order to check whether hyper-turbid conditions are possible, the research team, in particular Yoeri Dijkstra, studied the conditions under which hyper-turbidity may occur with an iFlow model, and reported his findings over two memos. The highlights and most practical aspects of these memos are discussed in detail in section 3.

In section 3, the iFlow model is briefly introduced and the results of a number of iFlow[1] simulations are summarized. In these simulations a parameter space is tested that is consistent with the physical considerations of section 2. These results do show stable hyper-turbid conditions. Later the settings and parameter space that were recommended – and that resulted in hyper-turbidity when modelled in iFlow – were tested in D3D. Section 4 is dedicated to the results of this new group of settings, when applied to D3D. Finally, conclusions and recommendations are in the last two sections.

[1] iFlow is an idealised process-based width-averaged model for systematic analysis of water motion and sediment transport processes in estuaries and tidal rivers (Dijkstra, Brouwer, Schuttelaars, & Schramkowski, 2017). iFlow is further introduced in section 3.1.

2 Theoretical considerations for hyper-turbidity

The conditions under which hyper-turbidity may occur were studied by Dijkstra in two memos, which are annexes to this report:

- "Choosing the right parameter space for 2DV Delft 3D hyper-turbidity simulations";
- "Ideas on the sediment availability in the idealised Delft 3D hyper-turbidity study";

The first memo presents a theoretical framework where the parameters that dominate vertical exchange of sediment are studied. As a conclusion of this study he defines a parameter space within which hyper-turbidity could occur. The second memo discusses the necessity of having enough availability of sediment over the estuary, so that the flow can erode it and bring it to the water column. The conclusion is that two processes, being resuspension (how much can be eroded) and trapping (controlling the availability of sediment) determine whether at a location hyper-turbid conditions can occur.

Formulated differently: High sediment concentrations in estuaries need two conditions:

1. the flow (tide and river discharge) must be strong enough to erode sediment from the bed;
2. sediment trapping at the estuary by along-channel trapping processes should be strong enough to bring and keep large amounts of sediment in suspension. This is the result of a combination of the estuarine configuration (convergence, depth, etc.), the sediment supply and hydrodynamic conditions.

Dijkstra formulated two dimensionless numbers that can function as indicator for each condition: the *dimensionless erosion parameter* and the *erodibility* ratio. These dimensionless numbers will be introduced in sections 2.1 and 2.2 respectively.

2.1 Condition for hyper-turbidity 1: dimensionless erosion parameter

The dimensionless erosion parameter indicates whether the erosive capacity of the flow and the bed erosion properties limit the near-bed concentration. In other words, this parameter quantifies whether the vertical exchange parameters between water and bed can lead to large near-bed concentrations. Its description in this section is based on (Dijkstra, Schuttelaars, & Winterwerp).

In equilibrium, under tidal-averaged conditions and assuming an abundant supply of sediment from the bed, deposition and erosion are in balance. Using the standard Delft3D erosion formulation and the Richardson & Zaki (1954) hindered settling formulation, we arrive to the following balance equation for the vertical exchange:

$$\langle w_s(\phi)\phi c_{gel} - M \max\left(\left(\frac{\tau}{\tau_c} - 1\right), 0\right)\rangle = 0, \qquad (1.1)$$

where the first term represents deposition of sediment and the second represents erosion. The brackets $\langle\ \rangle$ denote averaging over the tidal cycle. In the equation, the volumetric concentration $\phi = c/c_{gel}$, c is the sediment mass concentration, c_{gel} is the gelling concentration, M is the erosion parameter, τ is the bed shear stress and τ_c is the critical shear stress for erosion. The settling velocity is given by (Richardson & Zaki, 1954):

$$w_s = w_{s,0}(1-\phi)^5 \qquad (1.2)$$

Solving for the (dimensionless) near-bed concentration ϕ, equation 1.1 can be expressed in terms of a dimensionless erosion parameter $\tilde{E}$:

$$\tilde{E} = \frac{M}{c_{gel} w_{s,0}} \max\left(\left(\frac{\tau}{\tau_c} - 1\right), 0\right) \quad (1.3)$$

If $\tilde{E}$ is smaller than some threshold value $\tilde{E}_{thresh}$, the erosion capacity of the flow is limiting the concentration to ϕ_{bed} < 0.16. When $\tilde{E}_{thresh}$ is surpassed, concentrations larger than ϕ_{bed} = 0.16 can be attained near the bed. So, for example, if the gelling concentration is 100 g/L, concentrations up to 18 g/L can be attained near the bed when $\tilde{E}_{thresh}$ is reached. While these concentrations are high, they preclude a continuous transition between a potential fluid mud layer with concentrations of the order 100 g/L and the water column. Therefore, hyper-turbidity with exchange between the water column and a fluid mud layer, such as observed in the Ems, cannot remain stable in the model if $\tilde{E} < \tilde{E}_{thresh}$.

If $\tilde{E} > \tilde{E}_{thresh}$ the erosive capacity of the flow and the bed erosion properties are no longer limiting the concentration in the water column. The availability of sediment in the bed (and thus indirectly the sediment import) become the limiting factor. Hence hyper-turbid conditions become possible if there is enough erodible sediment in the bed.

For stationary flows $\tilde{E}_{thresh}$ = 0.067. For tidal flows, the value of $\tilde{E}_{thresh}$ depends on the turbulence and erosion-related parameters, but remains of the same order of magnitude. Therefore we will use $\tilde{E}_{thresh}$ = 0.067 as indicative value in this study.

Figure 2.1: Dimensionless erosion parameter $\tilde{E}$ versus the near-bed concentration $\phi = c/c_{gel}$ in equilibrium for stationary flows (copied from (Dijkstra, Schuttelaars, & Winterwerp)). The solid line denotes the maximum concentration that may be attained if the erosive capacity is limiting and if $\tilde{E} < \tilde{E}_{thresh}$(area I). The erosive capacity does not limit the concentration if $\tilde{E} > \tilde{E}_{thresh}$(area II). Similar figures may be derived for tidal flows, with somewhat different values for $\tilde{E}_{thresh}$.

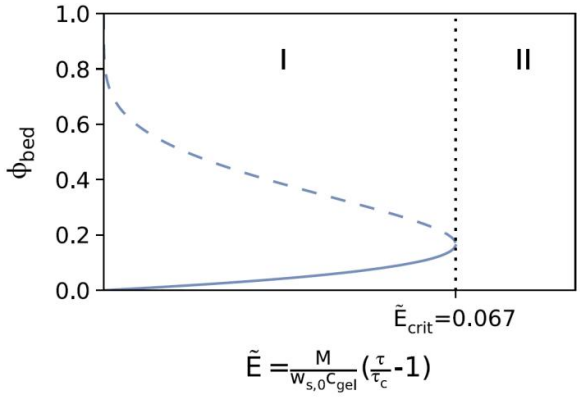

2.2 Condition for hyper-turbidity 2: sediment import and erodibility

The sediment importing capacity of an estuary depends on many processes and is therefore difficult to capture in a single parameter. Here we introduce the erodibility ratio as a representation of the sediment importing capacity. This parameter represents the amount of sediment available in the bed in the mouth, compared to the amount of sediment available in the bed in the ETM. Hyper-turbidity requires that there is much more sediment in the ETM than in the mouth and thus requires a high erodibility ratio.

In order to derive a mathematical expression for the erodibility ratio, we again start from the assumption of a tidal-averaged equilibrium. In equilibrium, the divergence of the sediment transport is zero, which means that there is zero net transport of sediment at every point of the estuary. Thus, the sediment concentration in the water column at equilibrium is determined by vertical exchange with the bed, yielding an expression similar to (1.1):

$$\langle w_s(\varphi_{bed}) c_{gel} \varphi_{bed} \rangle = \langle E \rangle,$$

where E represents the erosion flux. Different to (1.1) we no longer assume an abundant supply of sediment. The tidally-averaged erosion E can then be written as (Dijkstra, Schuttelaars, & Winterwerp)

$$\langle E \rangle = \langle M \max\left(\left(\frac{\tau}{\tau_c} - 1\right), 0\right)\rangle \; f,$$

where *f* is the tidally-averaged dimensionless *erodibility parameter*. In the standard bed model of Delft 3D the tidally-averaged erodibility follows from the mean sediment thickness in the bed, divided by the threshold thickness in a weighed time-average, i.e.

$$f = \frac{\langle \min\left(\frac{d_{sed}}{d_{thresh}}, 1\right) \hat{E} \rangle}{\langle \hat{E} \rangle}$$

If f equals zero there is no sediment in the bed during the entire tidal cycle. Hence, no erosion would occur. If f = 1, the amount of sediment on the bed exceeds the threshold thickness during the entire tidal cycle. If the amount of sediment on the bed exceeds the threshold thickness, the excess sediment does not add to an increased sediment concentration and hence becomes irrelevant. This means that erosion is at capacity conditions, determined by the bed shear stress, the erosion parameter and the critical shear stress. In this case the first condition (Section 2.1) is limiting the maximum concentration. For $0 < f < 1$ the tidally-averaged amount of available sediment is between zero and the threshold thickness. In this case, the total import of sediment (second condition, this section) limits the maximum concentration. If f_{ETM} and f_{sea} are the tidally-averaged dimensionless *erodibility parameter* at the ETM and at sea (respectively), the ratio of f_{ETM} compared to f_{sea} is the so-called *erodibility ratio.* This erodibility ratio gives insight into the erodibility of sediment at the turbidity maximum relative to that at the mouth (which is often prescribed, hence focus of our attention here). Strongly related to the erodibility ratio is the *availability ratio*, which is the ratio of the sediment thickness in the bed in the ETM and at the mouth $d_{sed,\ ETM}$ and $d_{sed,\ mouth}$. It is important to note that the erodibility ratio is closely related to the availability ratio, differing only by the fact that the erodibility is maximised at one. The results from Delft 3D in this report are analysed using the availability ratio, as this is somewhat easier to compute than the erodibility ratio and yields qualitatively similar results.

Following from both conditions, the sediment availability should be sufficiently large at a location where the shear stresses are large (relative to the bed erosion parameters) in order to obtain hyper-turbidity. This means that the sediment availability peak has to be at the middle of the estuary, where the shear stresses are the largest.

3 Testing physical considerations in iFlow

First a brief introduction to the iFlow model is given in section 3.1. A number of iFlow simulations were set up, aiming to test whether the theoretical conditions from section 2 can indeed result in the development of hyper-turbid conditions. Section 3.2 presents the results of these iFlow simulations.

3.1 iFlow model

iFlow is an idealised process-based width-averaged model for systematic analysis of water motion and sediment transport processes in estuaries and tidal rivers (Dijkstra, Brouwer, Schuttelaars, & Schramkowski, 2017). It is an analytical model that uses mathematical perturbation as solution method, thus providing very fast results. The results are typically the equilibrium tidal-averaged hydrodynamics and sediment distribution over the estuary. It is therefore ideal for sensitivity studies and used here to test the parameter space needed to sustain hyper-turbidity (and following the considerations presented in section 2.1 and section 2.2), as well as to obtain qualitative approximations of the sediment distribution over the estuary.

3.2 iFlow simulations and results

The iFlow simulations presented in this section were designed so that the two theoretical considerations from sections 2.1 and 2.2 are fulfilled. First, the sediment availability distribution over the estuary should be appropriate, i.e. maximum sediment availability around the middle of the estuary, where the shear stresses are largest. This can be done by increasing the convergence of the estuary, increasing the river discharge, and/or increasing the settling velocity of the sediments. A more converging estuary and a larger river discharge will help positioning the sediment availability peak towards the middle of the estuary, whereas the increased settling velocity will help in increasing the amount of sediment settling at this sediment availability peak (see report from previous phase, where increased settling velocity results in increased sediment thickness in the bed; simulation 3b, section 4.3.2).

The width convergence is therefore changed to L_b = 20 km and the depth becomes linearly sloping upwards from 6 m depth to 1.84 m (slope of $4 \cdot 10^{-5}$). As a result of these changes a decreasing water level amplitude in the last 50 km is observed (see annex note “AvailabilityD3Dproject”). The latter will certainly result in limited transport of sediment upstream over the last 50 km, and is consistent with the actual water level amplitude decay over the last 50 km of the Scheldt. This effect will be strengthened by an increased river discharge, resulting in a more optimal location of the sediment availability peak. Moreover, the settling velocity is increased to 2.5 mm/s. Table 3.1 shows the input parameters for the iFlow simulation. Figure 3.1 shows the sediment erodibility relative to the estuary mouth as obtained with iFlow after implementing these changes. It shows that one of the conditions for the development of hyper-turbidity is fulfilled, given the abundant sediment availability in the middle of the estuary (condition 2; section 2.2).

Parameter	Description	Value	Unit
H	**Depth**	**6**	**m**
$\boldsymbol{B_0}$	**Width at the mouth**	**3**	**km**
$\boldsymbol{L_b}$	**Exponential convergence length**	**20**	**km**
z_0^*	Dimensionless friction height (iFlow model)	$1*10^{-4}$	(-)
A_{M2}	M_2 amplitude at the mouth	2.13	m
A_{M4}	M_4 amplitude at the mouth	0.14	m
φ_{M2}	M_2 phase at the mouth	91	deg
φ_{M4}	M_4 phase at the mouth	179	deg
Q	River discharge	30	m^3/s
w_s (m/s)	Fall velocity	0.0025	m/s
K_h	Background diffusivity (sediment model)	100	m^2/s

Table 3.1: Input parameters of iFlow simulations

Figure 3.1. Sediment erodibility (with respect to erodibility at the mouth) for the new iFlow simulation with higher convergence, larger river discharge, and larger settling velocity.

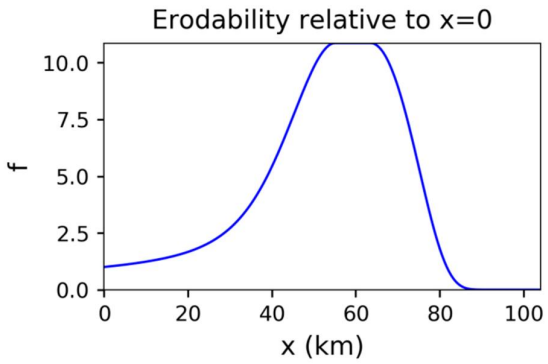

Next, the suspended sediment concentration was computed with iFlow. The sediment availability distribution from Figure 3.1 should result in hyper-turbidity when combined with the correct erosive settings. In order to demonstrate this, two iFlow simulations were performed where $\tilde{E}$ is larger than the theoretical 0.067 threshold:

- iFlow simulation 1 with parameter settings such that $\tilde{E} \approx 0.088$.
- iFlow simulation 2 with parameter settings such that $\tilde{E} \approx 0.132$.

The only difference between the simulations is in the erosion parameter M, which was 0.002 g/L m/s in simulation 1 and 0.003 g/L m/s in simulation 2. All other parameters remained as presented in table 3.1. For both simulations, the erosion capacity of the flow is no longer limiting the concentration, since $\tilde{E}$ > 0.067.

The results of the iFlow simulations are shown in Figure 3.2 to Figure 3.7. For simulation 1 the maximum near-bed concentration is about 12.5 g/L and the erodibility ratio at ETM relative to the mouth is about 10.5. For simulation 2 the maximum near-bed concentration is about 18.0 g/L and the erodibility ratio at ETM relative to the mouth is about 15.5. Both simulations show abundance of sediment for being eroded at the location where the shear stresses are typically larger in an estuary.

iFlow simulation 1

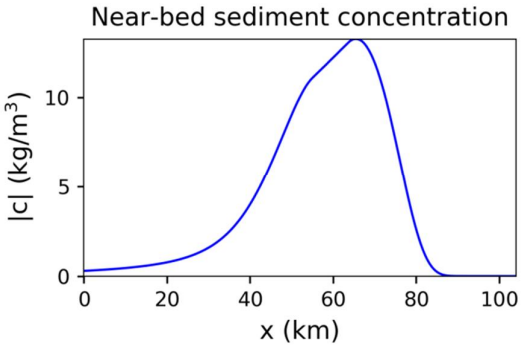

Figure 3.2: Near-bed sediment concentration over the estuary from iFlow simulation 1

iFlow simulation 2

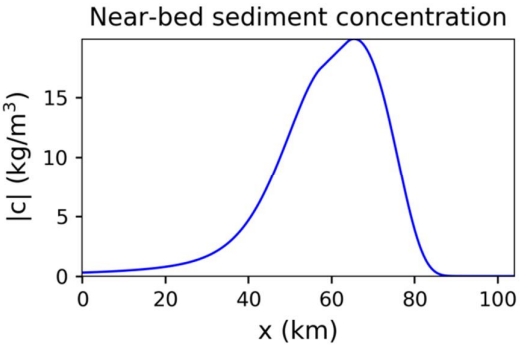

Figure 3.3: Near-bed sediment concentration over the estuary from iFlow simulation 2

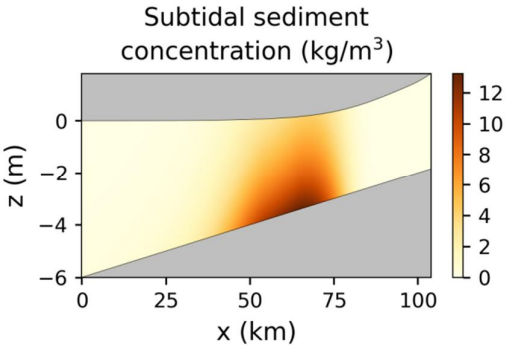

Figure 3.4: Vertical profile of sediment concentration over the estuary for iFlow simulation 1

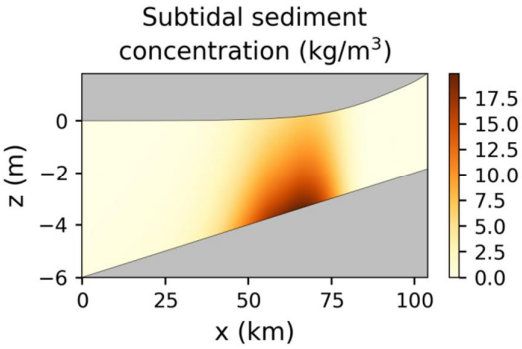

Figure 3.5: Vertical profile of sediment concentration over the estuary for iFlow simulation 2

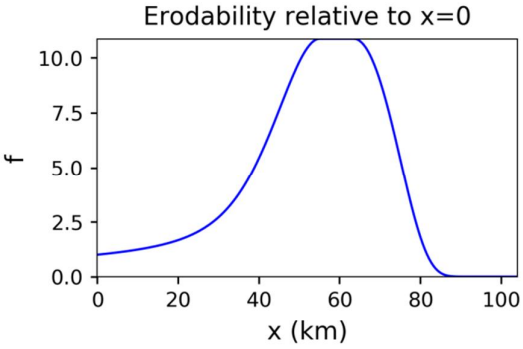

Figure 3.6: Erodibility over the estuary (relative to the mouth) for iFlow simulation 1

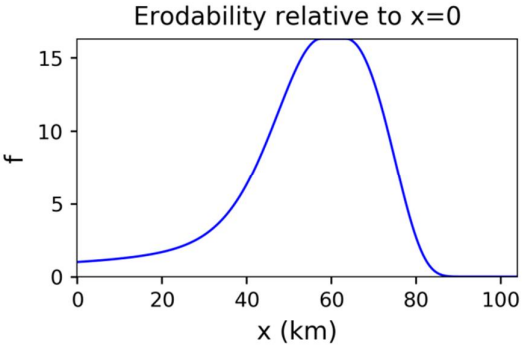

Figure 3.7: Erodibility over the estuary (relative to the mouth) for iFlow simulation 2

To conclude, the dimensionless numbers that were formulated to fulfil the necessary conditions for hyper-turbidity helped gaining insight into the parameter space for which hyper-turbidity can be attained with iFlow.

4 D3D results incorporating physical considerations and considering iFlow results

Section 3 demonstrated that an iFlow model can be set up that results in hyper-turbid conditions by incorporating the physical considerations from section 2. Following up the promising results obtained in iFlow a new set of simulations was performed in D3D, also incorporating these physical considerations. The results of these simulations are described in this section.

For the first two simulations of this new set, only sediment transport parameters were modified, leaving model forcing and convergence identical to the previous phases of the project. The focus was to affect the vertical exchange equilibrium, hence the dimensionless erosion parameter (see section 2.1). This was done for both model configurations 3 and 5 of the previous phase of the project. The results from this group of new simulations serve as example that 'it is not enough to find the optimal vertical exchange parameters settings if not accompanied by the adequate changes in model convergence - configuration (and hence sediment availability)'.
For all other simulations, both sediment parameters and model configuration (convergence, river discharge, etc.) were modified. The starting point for these modifications was model configuration 3, which means that the new model configuration contains the standard D3D bed model (and not the buffer layer model as model configuration 5).

Model configuration	*simulation name*	*Section 3.3 equivalent*	w_s *(m/s)*	$\tau_{c,b}$ *(Pa)*	τ_{mean} *(Pa)*	M *(kg/m^{2}s)*	*convergence*	*river discharge (m^3/s)*	$\widetilde{E}$*(-)*
3	3f		0.0005	0.2	2	0.0005	standard	30	**0.180**
5	5g		0.001	0.2[2]	2	0.0001[3]	standard	30	**0.108**
6	6a		0.0025	0.2	1.3	0.0005	stronger	70	0.022
6	6b		0.0025	0.2	1.3	0.001	stronger	70	0.044
6	6c	1	0.0025	0.2	1.3	0.002	stronger	70	**0.088**
6	6d	2	0.0025	0.2	1.3	0.003	stronger	70	**0.132**
7	7a		0.001	0.2	1.3	0.0005	stronger	70	0.055
7	7b		0.001	0.2	1.3	0.0003	stronger	70	0.033
7	7c		0.001	0.2	1.3	0.0004	stronger	70	0.044
7	7d		0.001	0.2	1.3	0.00035	stronger	70	0.038
7	7e		0.001	0.2	1.3	0.0015	stronger	70	**0.165**
7	7f		0.001	0.2	1.3	0.00045	stronger	70	0.049
8	8a		0.0005	0.2	1.3	0.0005	stronger	70	**0.110**
8	8b		0.0005	0.2	1.3	0.001	stronger	70	**0.220**
8	8c		0.0005	0.2	1.3	0.0002	stronger	70	0.044

Table 4.1. Overview of D3D simulations during the current phase of the project.

[2] Of the fluffy layer, the τ_c of the bed was 1 Pa, see previous phase report for more details.
[3] Of the bed, the M of the fluffy layer was 0.03 s/m, see previous phase report for more details.

An overview of all simulations can be found in table 4.1. c_{gel} is kept as 50 g/l for all simulations, and thus excluded from the overview.

To improve our understanding, the potential to obtain hyper-turbid conditions in the simulations of the previous phase of the project is described in section 4.3.

4.1 Results from the simulations with only adjusted sediment parameters (condition 1 only)

The first two simulations listed in table 4.1, simulations 3f and 5g (consistent and therefore comparable with the nomenclature at the previous phase of the project), are the only two new simulations that were performed on former model configurations. Only sediment parameters were modified, aiming to obtain a $\tilde{E}$ > 0.067.

Table 4.1 shows that the new sediment parameters are such that indeed $\tilde{E}$ > 0.067 is achieved. However, this does not lead to the development of hyper-turbid conditions. Figure 4.1 and Figure 4.3 show that a maximum SSC of less than 1 g/l was achieved. This is explained by the fact that, though the erosive settings and forcing were favourable to develop hyper-turbidity (condition 1, section 2.1), the sediment availability in the bed was small (condition 2, section 2.2). Therefore the limiting factor of the erosion from the bed and the resulting SSC are also small. This is shown in Figure 4.2 and Figure 4.4, where the sediment in the bed at the end of the simulation period can be observed. The sediment is available for erosion only in the upstream part of the river, hence not being available for erosion at the locations where the bed shear stresses are largest. Thus, the current configuration of the estuary results in a sediment distribution over the estuary that limits the availability of sediment for erosion. The second condition for hyper-turbidity (section 2.2) is therefore not fulfilled.

Figure 4.1. Suspended sediment concentration over the estuary (at the end of the simulation period) for simulation 3f, where $\tilde{E}$ > 0.067.

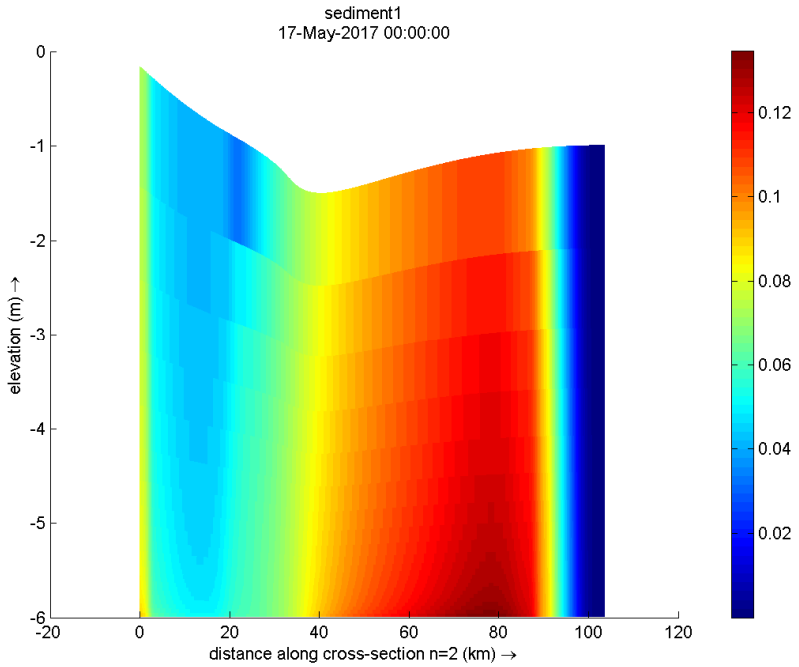

Figure 4.2. Sediment thickness over the estuary (at the end of the simulation period) for simulation 3f, where $\tilde{E}$ > 0.067.

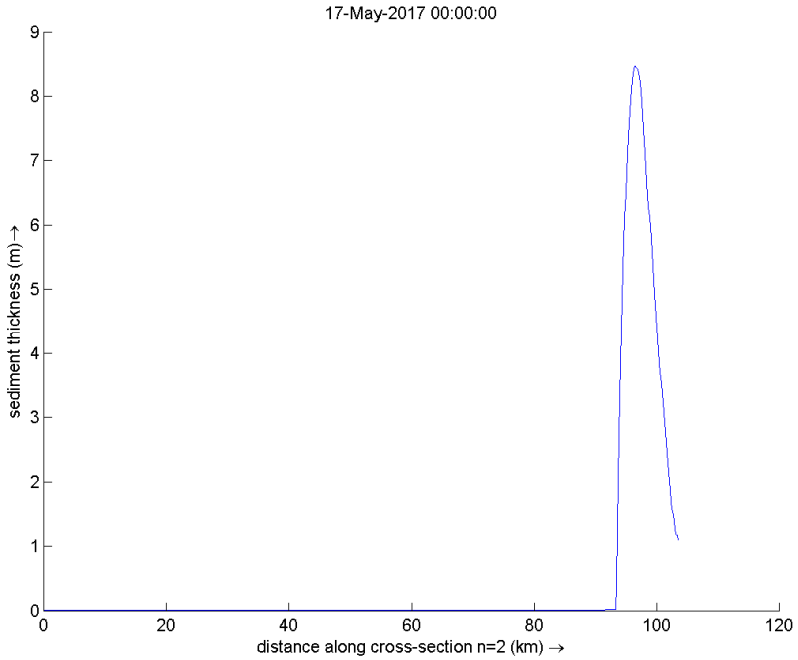

Figure 4.3. Suspended sediment concentration over the estuary (at the end of the simulation period) for simulation 5g, where $\tilde{E}$ > 0.067.

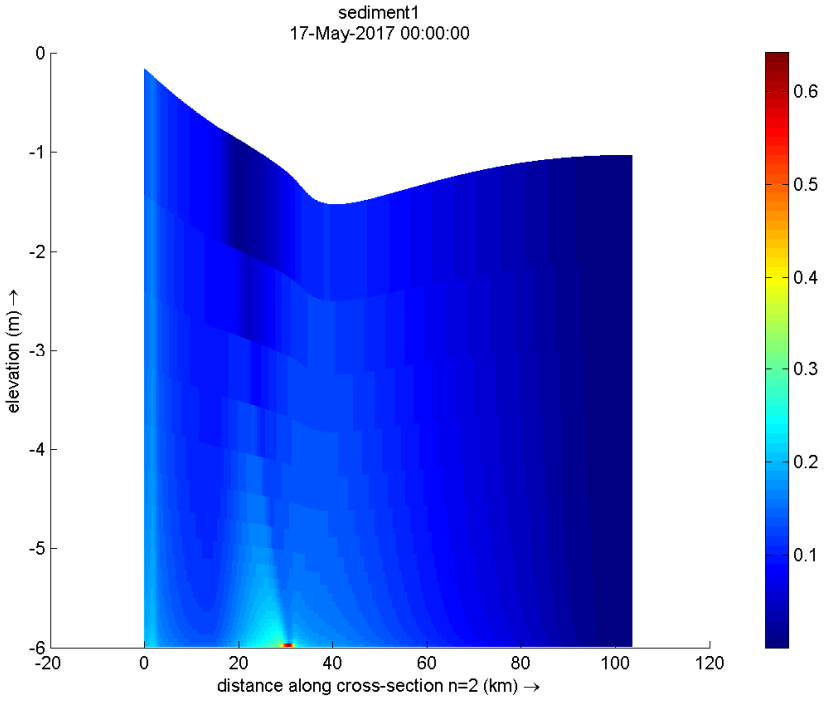

Figure 4.4. Available mass of sediment in the bed over the estuary (at the end of the simulation period) for simulation 5g, where $\tilde{E}$ > 0.067.

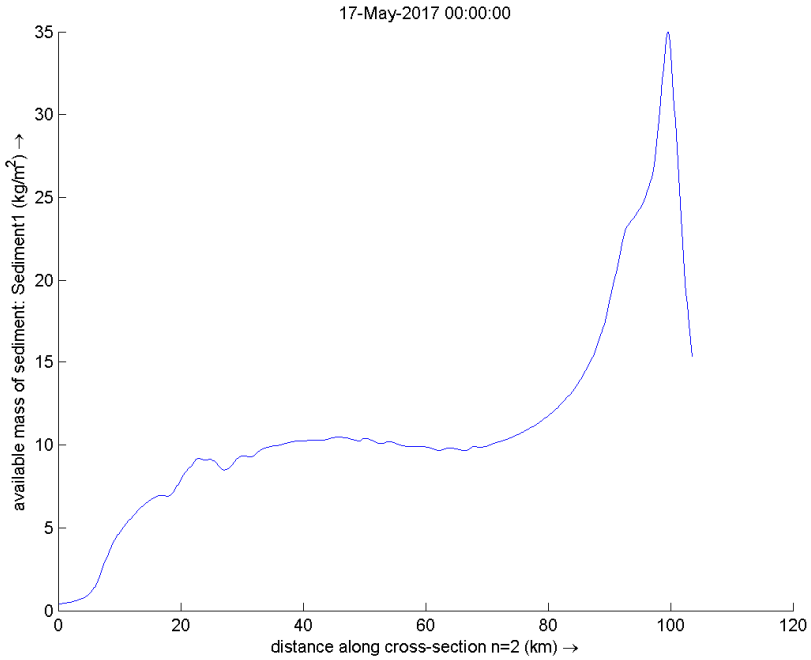

4.2 Results for the simulations with adjusted sediment parameters and model configuration (conditions 1 and 2)

Apart from the two simulations presented in section 4.1, all other new D3D simulations have a modified model configuration from the simulations carried out in the previous phases of the project. This new configuration consists of a) a width convergence of L_b = 20 km, b) a depth linearly sloping upwards from 6 m depth to 1.84 m (slope of $4 \cdot 10^{-5}$), and c) a river discharge of 70 m^3/s. This is the same model configuration as the one tested in iFlow (as presented in section 3.2), which resulted in hyper-turbidity. Moreover, all the new D3D simulations were grouped into model configurations attending to the settling velocity that was used. Three different settling velocities were tested, resulting in: model configuration 6 (following numbering from previous phase of the project) for a settling velocity of 2.5 mm/s; model configuration 7 for a settling velocity of 1 mm/s; model configuration 8 for a settling velocity of 0.5 mm/s. The background for grouping different settling velocities into different model configurations is the fact that the settling velocity affects substantially the trapping capacity of the estuary as explained in section 3.3 and demonstrated in the note "AvailabilityD3Dproject" and the previous report of this project in section 4.3.2.

Figure 4.5 shows the sediment availability at the ETM to the sediment availability at the mouth ratio plotted against $\tilde{E}$ for model configuration 6. The latter was obtained by dividing the sediment thickness at the ETM by the sediment thickness at the mouth as provided by D3D, and is therefore not exactly the erodibility ratio shown in section 3.3, which is direct output from iFlow. Nevertheless, the sediment availability ratio shows consistency with the information provided by the erodibility ratio as in section 3.3, and confirms sediment abundance at the ETM relative to the estuary mouth. This suggests that there is enough sediment in the bed around the location where the erosive forces are the largest. Moreover, Figure 4.5 shows sediment

availability ratios that increase for increasing $\tilde{E}$. The latter is attributed to the larger vertical exchange of sediment between bed and water column, which favours tidal asymmetry in sediment concentration and therefore increases the import of sediment into the estuary. Note that tidal asymmetry is the dominant importing mechanisms in this schematized estuary (see the note "AvailabilityD3Dproject"). Before $\tilde{E}$ reaches the theoretical threshold defined in section 2.1, the availability ratio starts increases linearly with $\tilde{E}$. However, when the theoretical threshold for $\tilde{E}$ of 0.067 is surpassed, the availability ratio starts increasing exponentially.

Figure 4.6 shows the maximum observed suspended sediment concentration over the tidal cycle plotted against $\tilde{E}$ for model configuration 6. This maximum observed concentration is characterized by the concentration of the fluid mud layer right after the collapse of the water column. The maximum observed suspended sediment concentration was found to be a good proxy to characterize sediment concentrations from the simulations. Further details on suspended sediment concentration dynamics and characteristics will be presented in section 4.3. As Figure 4.6 shows, the maximum SSC increases exponentially once the theoretical threshold of $\tilde{E}$ > 0.067 is surpassed, attaining 10 g/l and larger. This is consistent with the iFlow findings presented in section 3.2 (Figure 3.2 and Figure 3.3), where the first simulation (equivalent to simulation 6c, see table 4.1) and second simulation (equivalent to simulation 6d, see table 4.1) exhibited maximum sediment concentrations (averaged over the tidal cycle) of about 12 and 17 g/l respectively. Note that, as shown in Figure 4.6, the D3D equivalents of these iFlow (simulations 6c and 6d, see table 4.1) display larger maximum concentrations. However, the sediment concentrations reported in Figure 4.6 are the maximum over every tidal cycle, whereas the sediment concentrations obtained for iFlow are averaged over the tidal cycle. Sediment concentration profiles over the vertical for model configuration 6 will be presented in section 4.3, enabling a clearer comparison with the (averaged) sediment concentration profiles as obtained in iFlow. Without going into details, it can be concluded that indeed the conditions for hyper-turbidity introduced in section 2 can be used to reproduce a hyper-turbid equilibrium in D3D, exhibiting comparable results as when modelled with iFlow. Please note that the transition towards hyper-turbidity was not simulated in D3D, but only the equilibrium hyper-turbid conditions themselves.

Now that the applicability of the theory to arrive to hyper-turbidity has been demonstrated in both iFlow (section 3.2) and D3D (this section), the impact of the model configuration (via de settling velocity parameter) on the observed sediment concentration can be elaborated upon. As already stated, the settling velocity strongly influences the trapping capacity of the estuary (e.g. the capacity of accumulating sediment). Figure 4.7 shows the sediment availability at the ETM to the sediment availability at the mouth ratio plotted against $\tilde{E}$ for model configuration 7, with the results from model configuration 6 being plotted in grey for reference. The only difference with model configuration 6 is a smaller settling velocity, of 1 mm/s (in contrast to the settling velocity of 2.5 mm/s of model configuration 6). The results from model configuration 7 show also increasing sediment availability ratios for increasing $\tilde{E}$ for the lower range of studied $\tilde{E}$ values. However, once $\tilde{E}$ increases beyond 0.045, the sediment availability ratio starts to decrease. We hypothesize that the latter occurs because of the transition from erosion limited conditions (when large sediment concentrations in the water column cannot be reached because the erosion parameters are not large enough) to supply limited conditions (when large sediment concentrations in the water column cannot be reached because sediment is eroded from the bed faster than is supplied to the bed by advection processes from elsewhere in the estuary and outside the estuary). In model configuration 6, the large settling velocity forced an important amount of the sediment entering the estuary to remain on the bed. In other words, the sediment was trapped in the estuary. On the other hand, in model configuration 7, the

smaller settling velocity results in less sediment being trapped. Sediment did enter the estuary anyway, but (given its smaller settling velocity) it did not have time to settle before the tidal motion flushed it away from the estuary again. This resulted in less sediment in the bed. So, once the erosive forces were large enough (or once the erosion parameters are such that these favour erosion), conditions were supply-limited.

Figure 4.8 shows the maximum observed suspended sediment concentration over the tidal cycle plotted against $\tilde{E}$ for model configuration 7, with the results from model configuration 6 being plotted in grey. Again, in the lower ranges of $\tilde{E}$, when it remains smaller than 0.045, the observed suspended sediment concentrations are very similar to these from model configuration 6. However, once a certain threshold is surpassed, suspended sediment concentrations increase rapidly. This is followed by a sudden decrease well below the values from model configuration 6. The initial increase in suspended sediment concentration can be explained by the positive effect of a decrease in settling. If erosion is stronger, the smaller settling velocity (than in model configuration 6) unbalances the vertical equilibrium, favouring the erosive forces. These dominate the settling process, resulting in larger suspended sediment concentrations. (This can be clearly observed when comparing SSC for model configuration 6 and 7 at $\tilde{E}$=0.044). However, the effect of the decreased settling velocity holds only for a small increase of $\tilde{E}$. Soon after a further increase of $\tilde{E}$, the smaller trapping capacity of the estuary, as a result of a smaller settling velocity, becomes dominant. The net result is that sediment is eroded from the bed before being supplied. This results in empty beds (as shown in Figure 4.7) and small sediment concentration (as shown in Figure 4.8). The sediment arriving to the bed is quickly eroded from it, and transported elsewhere again. This combination of large erosive settings and small settling velocity behaves as a system where settlement of sediment in the bed is not allowed: sediment comes in and out of the estuary, but does not settle in the bed hence not being available for re-suspension.

Figure 4.5. Sediment availability ratio for model configuration 6, with stronger convergence, larger river discharge, and a settling velocity of 2.5 mm/s. The other sediment parameters are varied to produce the increasing E values.

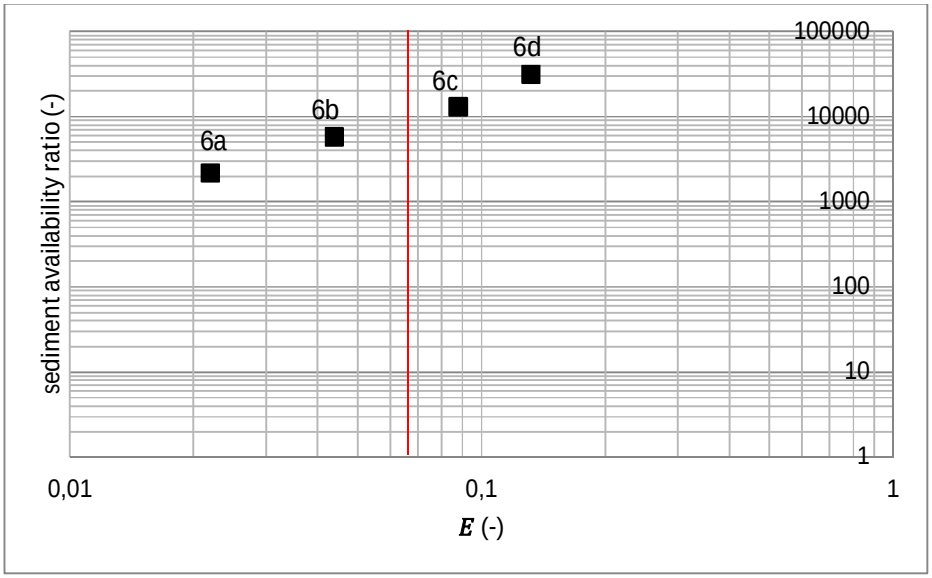

Figure 4.6. Maximum suspended sediment concentration for model configuration 6, with stronger convergence, larger river discharge, and a settling velocity of 2.5 mm/s. The other sediment parameters are varied to produce the increasing E values.

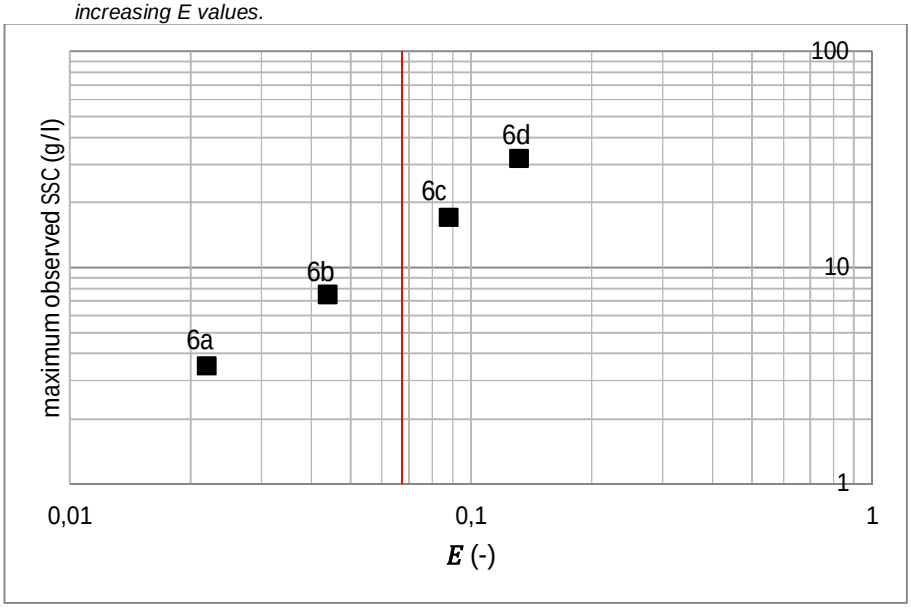

Figure 4.7. Sediment availability ratio for model configuration 7, with stronger convergence, larger river discharge, and a settling velocity of 1 mm/s. The other sediment parameters are varied to produce the increasing E values. The values from model configuration 6 (Figure 4.5) are plotted in grey as a reference.

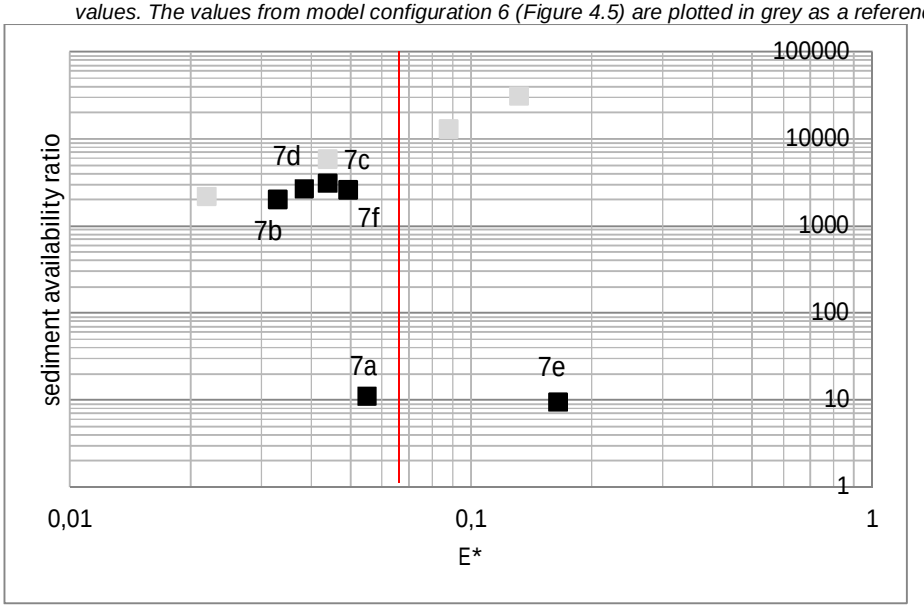

Figure 4.8. Maximum suspended sediment concentration for model configuration 7, with stronger convergence, larger river discharge, and a settling velocity of 1 mm/s. The other sediment parameters are varied to produce the increasing E values. The values from model configuration 6 (Figure 4.5) are plotted in grey as a reference.

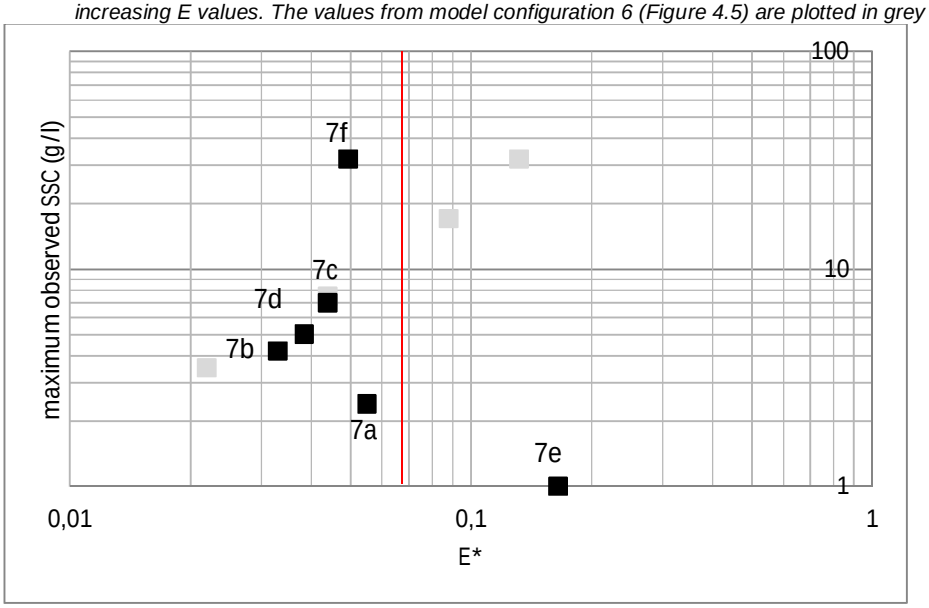

Finally, Figure 4.9 and Figure 4.10 show the sediment availability ratio and the maximum observed SSC for model configuration 8 simulations. Note the several orders of magnitude mismatch with the y-axis scales from Figures 4.7 and Figure 4.5. Model configuration 8 is characterized by smaller settling velocity than in model configurations 6 and 7. This means smaller trapping capacity and associated smaller sediment availability ratio at the ETM. Figure 4.5 and Figure 4.7 showed sediment availability ratios at the ETM in the order of 1000, with only the two simulations exhibiting supply limited conditions (7a and 7e) having similar sediment availability ratios to these from model configuration 8. This suggests that model configuration 8 always results in supply limited conditions. The maximum SSC from model configuration 8 also remain as low as the maximum SSC reported for supply limited conditions simulations at model configuration 7. Finally, there seems to be a positive effect in sediment availability ratio and maximum observed SSC when increasing $\tilde{E}$ beyond the threshold of 0.067, but this effect is irrelevant for the development of hyper-turbid conditions.

Figure 4.9. Sediment availability ratio for model configuration 8, with stronger convergence, larger river discharge, and 0.5 mm/s settling velocity. The other sediment parameters are varied to produce the increasing E values.

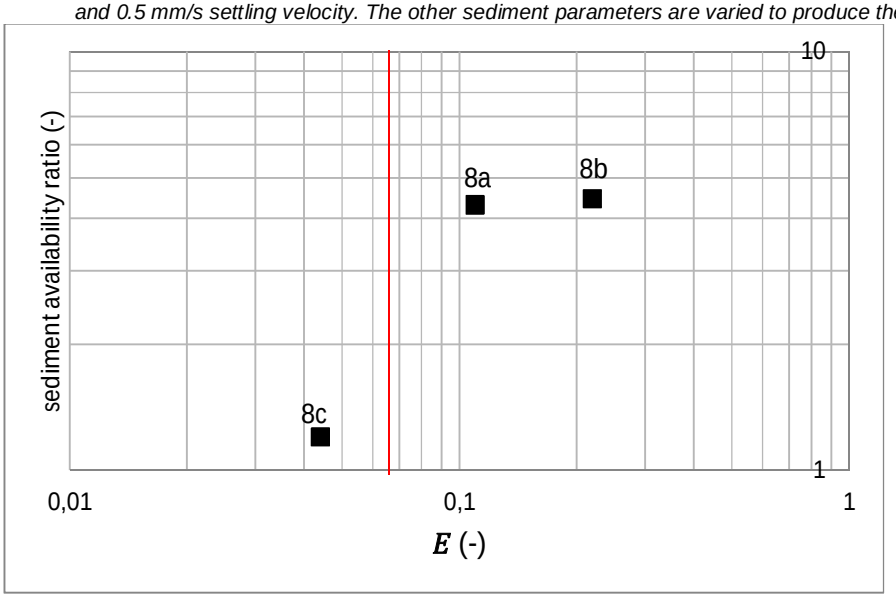

Figure 4.10 Maximum suspended sediment concentration for model configuration 8, with stronger convergence, larger river discharge, and 0.5 mm/s settling velocity. The other sediment parameters are varied to produce the increasing E values.

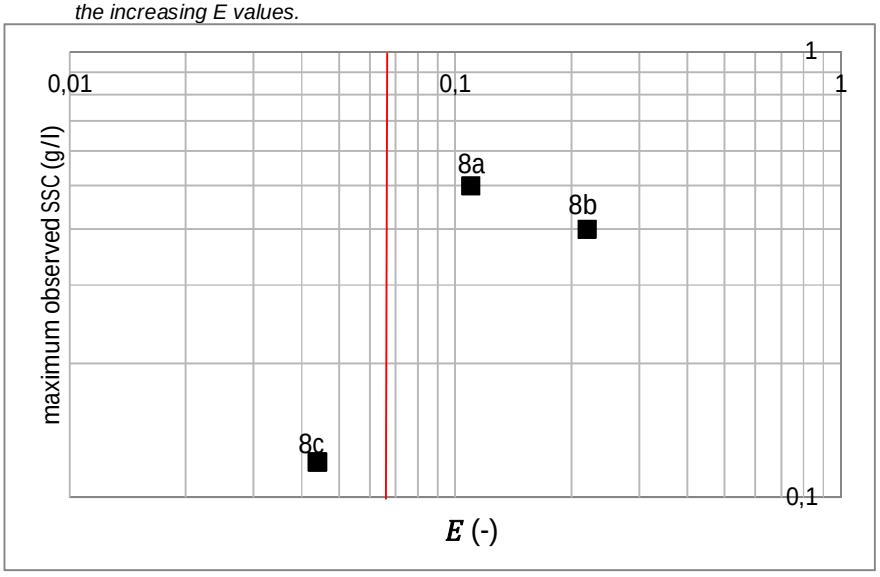

4.3 Detailed hyper-turbidity results

This section elaborates on the results of the simulations presented in section 4.2 and listed in table 4.1 that led to hyper-turbid conditions.

From all the studied cases, the clearest example of hyper-turbid conditions was simulation 6d. Figure 4.11 shows the suspended sediment concentration in the estuary at equilibrium for simulation 6d, where $\tilde{E} > 0.067$ and the trapping capacity of the estuary is the largest tested. At this particular snapshot, the SSC exceeds 1.5 g/l at approximately 60% of the water column

over 5 km of estuary. Peaks of 4 g/l also occur over the same length, but close to the bed. A SSC close to 1 g/l is exhibited throughout the whole water column between km 40 and km 65. This sort of prevailing large SSC were not observed so far for the current project.

Figure 4.11 Suspended sediment concentration over the estuary (at the end of the simulation period = equilibrium?) for simulation 6d, where $\tilde{E}$ > 0.067 and the trapping capacity of the estuary is the largest tested.

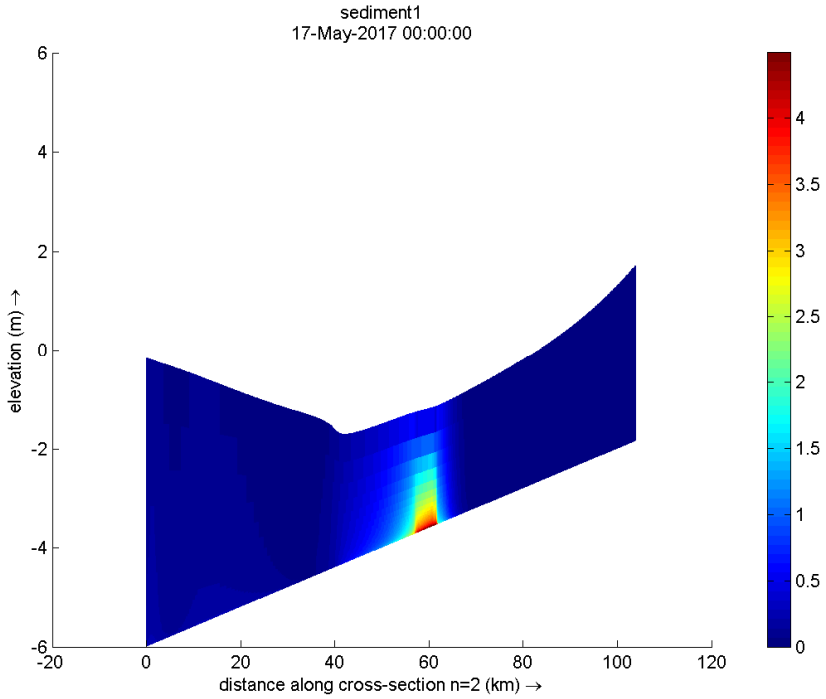

Figure 4.12 shows results from the same simulation (6d), but at a time step where even larger SSC concentrations are exhibited over a large portion of the water column. We could consider this snapshot as characteristic for the largest well mixed suspended sediment concentrations. Concentrations larger than 5 g/l are observed over 4 m of water column and 5 to 10 km in the estuary. At the water surface, concentrations up to 2.5 g/l are observed. Concentrations of 1 g/ or morel are found over the majority of the water over at least 30 km estuary.

Figure 4.13 completes the overview of suspended sediment concentration over the estuary at different time steps for simulation 6d. It shows the development of a fluid mud layer on the bed of the estuary. The Figure captures the development of a fluid mud layer after the collapse of the water column, and shows concentrations larger than 25 g/l.

Figure 4.12 Suspended sediment concentration over the estuary (when the observed concentrations are the largest) for simulation 6d, where $\tilde{E}$ > 0.067 and the trapping capacity of the estuary is the largest tested.

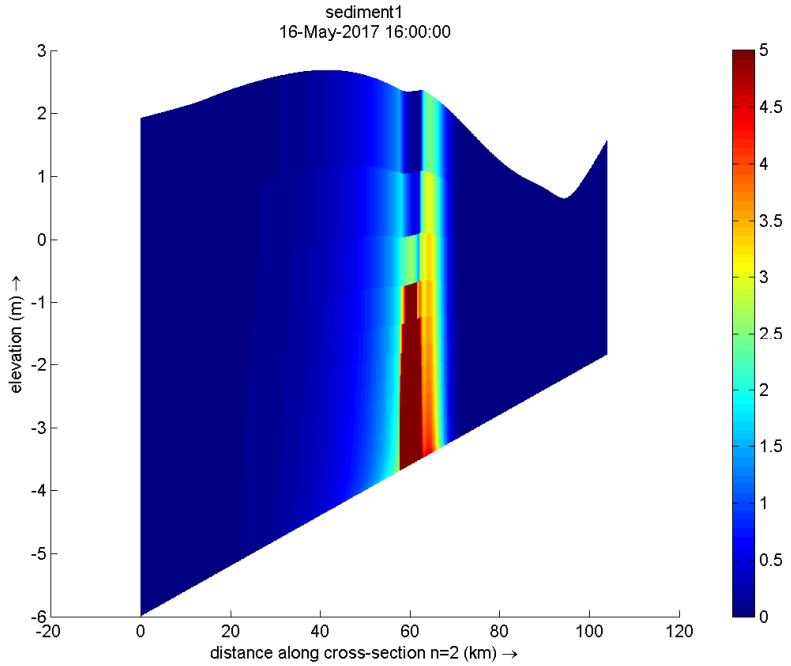

Figure 4.13. Suspended sediment concentration over the estuary (when the observed concentrations are the largest) for simulation 6d, where $\tilde{E}$ > 0.067 and the trapping capacity of the estuary is the largest tested.

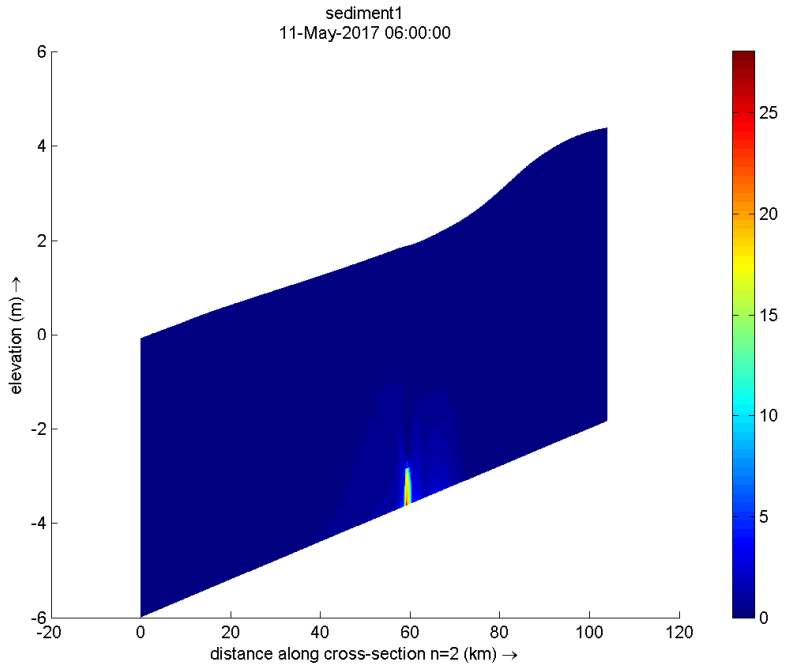

It is important to note that in the earlier work was demonstrated that the equilibrium SSC at our schematized D3D estuary is independent from the initial sediment thickness in the bed. Still, one extra simulation was performed in the current phase to demonstrate that this still holds, even for the current type of highly turbid final equilibrium states. The simulation with no sediment in the bed initially exhibited identical results as the simulation with initial abundance of sediment in the bed.
The conclusion is that what has been reported so far does not depend on the initial presence of sediment in the bed.

Figure 4.14 shows the cumulative total transport of sediment at the cross-sections at 5 km, 25 km, 30 km, and 50 km. The cumulative flux at the cross section at 75 km is also plotted (in black). The figure shows that, after some spin-up time in which a lot of the initially present sediment in the bed is washed away, the rate of import of sediment is constant through all cross sections until arriving to the ETM (the slope of all lines is parallel). At the ETM the rate of import drops to zero. This means that sediment entering the estuary ends up depositing below the ETM, without being deposited anywhere else in the river.

Figure 4.15 shows the bed thickness over the estuary, where a layer of sediment in the bed of more than 20 m can be observed around km 60, right below the location of the ETM. Note that in the model sediment accumulation in the bed does not lead to changes of the bed level. The stretch of river from the estuary mouth to the point where sediment accumulates is empty. Therefore, we have supply limited conditions up until the point where sediment accumulates. The sediment supplied by the estuary is not enough to meet the demand from the erosive forces. Around the location of the ETM, supply becomes larger than the demand for erosion, and sediment accumulates. Note that in D3D there is no intermediate point between an empty bed and a bed that accumulates infinitely, at least not for a situation with constant forcing (as the modelled one). Also, note that in D3D erosion of the bed is a function of the bed thickness when the thickness is smaller than 5 cm (see threshold thickness at section 2.2), and becomes independent of the bed thickness for larger thicknesses. Thus the model cannot “feel” the difference between a 6 cm and a 10 m sediment layer in the bed and therefore erosion fluxes remain constant despite the increased sediment thickness. Variations of the forcing (e.g. amplitude or period of the tide, spring-neap cycle and river discharge) would result in the migration of the spot where sediment accumulates in the bed. Therefore, under real (variable) forcing, we hypothesize that the sediment accumulation would be spread over a larger stretch of bed, arriving to a somehow more realistic sediment distribution in the bed. Moreover, the effect of fluid mud may contribute to increased SSC levels through fluid mixing.

Despite of the peculiar sediment accumulation pattern modelled in the bed, it is considered that the model captures the relevant mechanisms behind the development of hyper-turbidity, and delivers the expected results given the simplified nature of its forcing.

Figure 4.14. Cumulative total transport of sediment at the following cross-sections (in reds and magentas, from bottom to top as plotted in the figure): 5 km, 25 km, 30 km, and 50 km. The cumulative flux at the cross section at 75 km is also plotted in black.

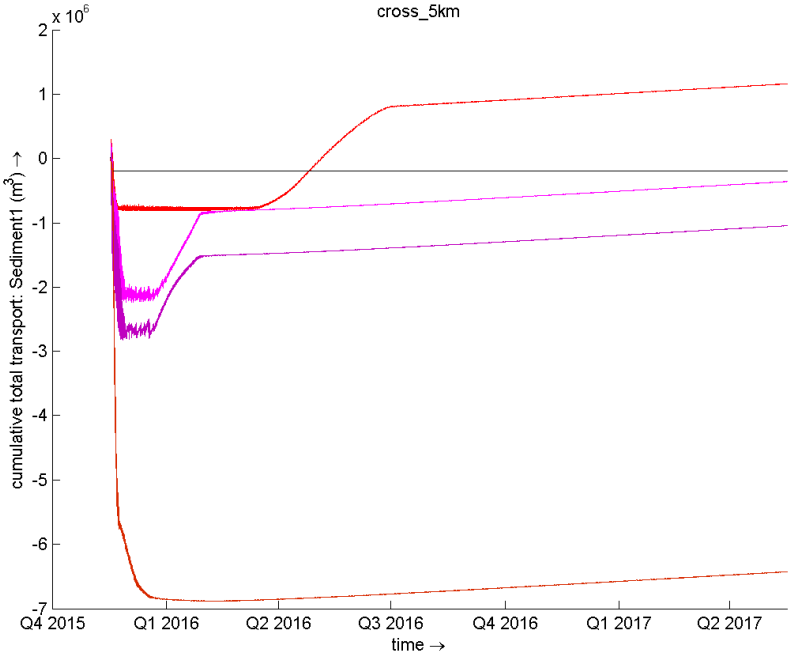

Figure 4.15. Sediment in the bed over the estuary (at the end of the simulation period) for simulation 6d, where $\tilde{E} >$ 0.067 *and the trapping capacity of the estuary the largest tested.*

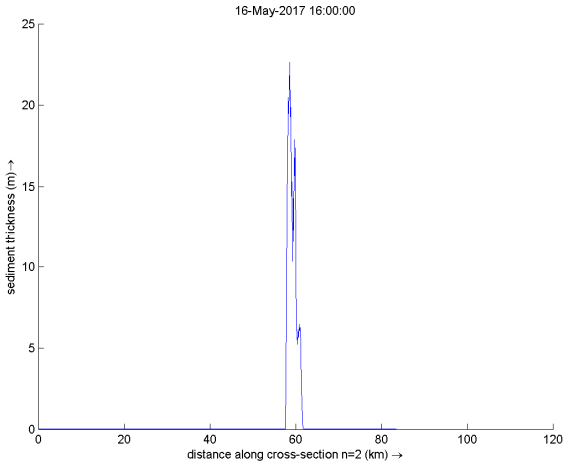

Figure 4.16 shows the total suspended sediments in the system for the complete simulation time, divided into sediments in the bed and suspended sediments. After the initial spin-up time of about 2 months, sediment gets continuously imported into the estuary and settles in the bed. The accumulation rate becomes constant once a layer of sediment that is always larger than 5 cm establishes in the vicinity of the ETM (in practice this is at around 40 km from the estuary mouth), and given the erosion behaviour presented in the previous paragraph. Also, total

suspended sediments in the system slowly arrives to equilibrium after a first initial increase caused by the erosion of the sediments at the initially uniform bed. The reason why the total suspended sediment in the system does not increase despite of the fluid mud layer on the bed (which causes tidal amplification as reported in the previous phase of the project) is because settling dominates from erosion in the vertical sediment exchange balance under the ETM, and despite the small increase in erosive forces caused by tidal amplification (see the following paragraphs of the current section for further information on tidal amplification effects).

Figure 4.16. Total suspended sediments in the system, divided into sediment in the bed and suspended sediments, for simulation 6d.

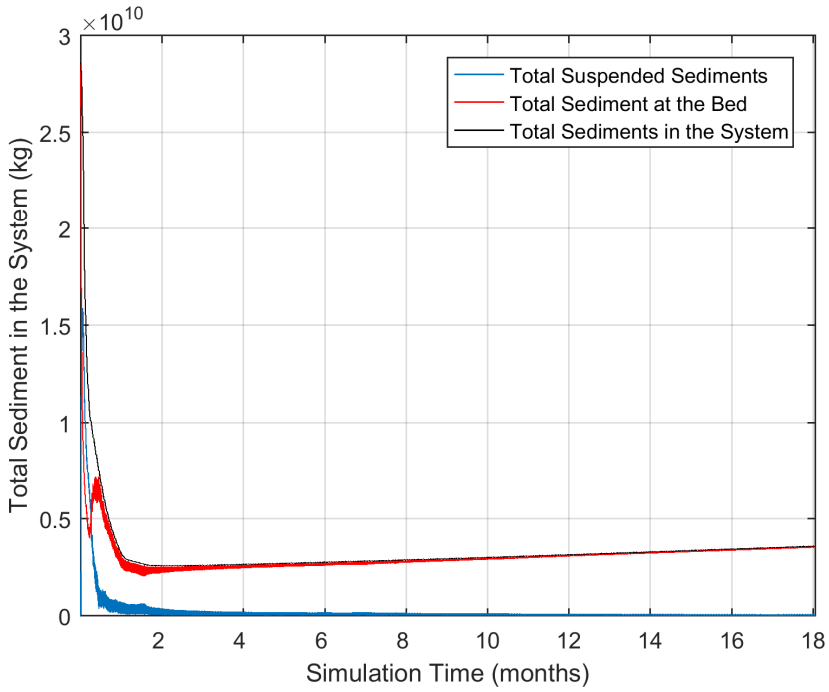

Next, we will present the results from simulation 6d, but in a model configuration where there is no effect of sediment in fluid density. In this way we will evaluate the role of the effect of sediment in fluid density in the development of hyper-turbid conditions. Figure 4.17 shows the sediment distribution over the water column at the end of the simulation for simulation 6d, but in a situation where sediment does not affect the fluid density. The suspended sediment concentration pattern has changed completely. First, the ETM is now located at the mouth of the estuary, with the SSC becoming almost zero at the point of maximum salinity penetration. Second, the magnitude of the ETM has also decreased substantially, with concentrations of 1g/l or larger only being reached over half of the water column and over less than 5 km of estuary. Figure 4.18 shows the sediment in the bed at the end of the simulation period for simulation 6d and no effect of sediment in fluid density. Sediment only accumulates over the first 20 km next to the mouth, and it never reaches thickness larger than 5 cm. Together, Figure 4.17 and Figure 4.18 draw a very different picture compared to the same simulation 6d, where the only difference was the effect of sediment in fluid density. Over the next paragraphs we elaborate on the mechanisms triggering these differences.

Figure 4.17 Suspended sediment concentration over the estuary (at the end of the simulation period) for simulation 6d (but with no effect of sediment in fluid density), where $\tilde{E}$ > 0.067 and the trapping capacity of the estuary is the largest tested.

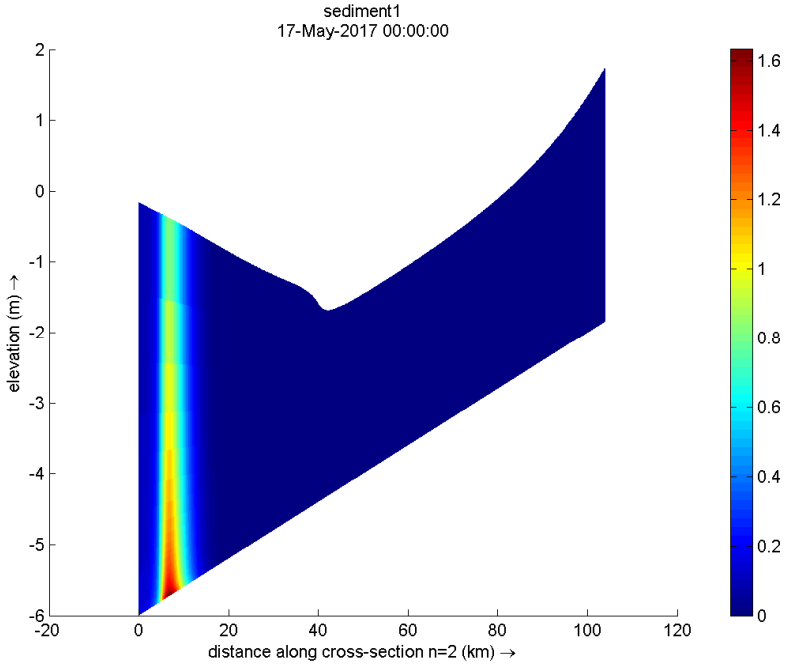

Figure 4.18 Available mass of sediment in the bed over the estuary (at the end of the simulation period) for simulation 6d (but for no effect of sediment in fluid density), where$\tilde{E}$ > 0.067and the trapping capacity of the estuary the largest tested.

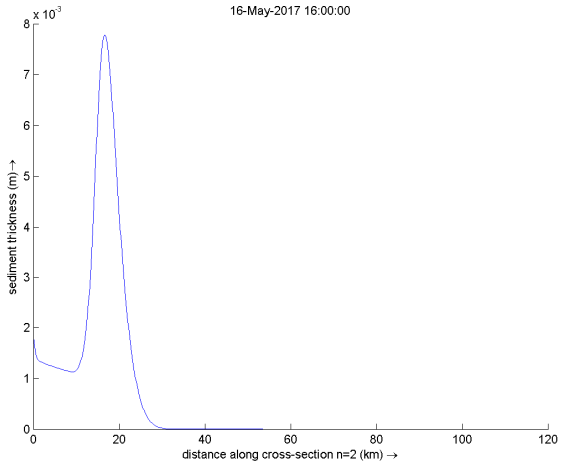

Figure 4.19 shows the vertical eddy viscosity profile in the proximity of the ETM for simulation 6d (in red), as well for the same simulation but without effect of fluid density (in blue). This plot is produced with the results of a time step close to the end of the simulation period, hence when sediment is abundant for simulation 6d (and absent for simulation 6d with no effect of

sediment in fluid density). Figure 4.19 shows that the turbulence is damped by a factor 3 when the effect of sediment in fluid density is activated. This results in the hydrodynamics shown in Figure 4.20 and Figure 4.21. When turbulence is damped, larger average flow velocities (10 cm/s faster at maximum flow velocity for this particular snapshot) are observed over the estuary (Figure 4.20), as well as higher water levels (20 cm larger in this case; Figure 4.21). These favour import of sediment into the estuary, and become an important factor to develop hyper-turbidity in this schematized example.

Figure 4.19. Vertical eddy viscosity at a location close to the ETM for simulation 6d with effect in fluid density (in red), and without effect in fluid density (in blue).

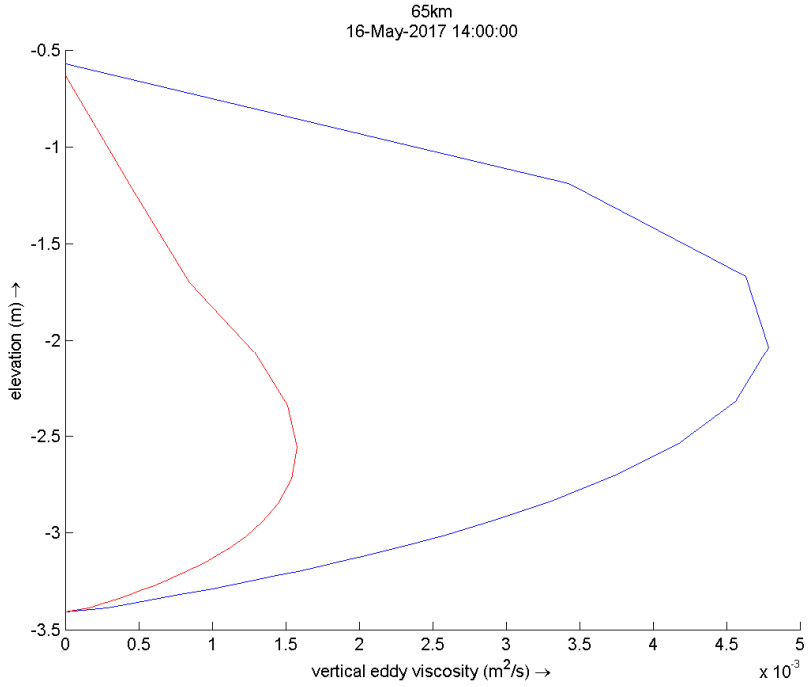

Figure 4.20. Depth averaged velocity over the estuary for simulation 6d (in red), and for the same simulation, but with no effect in fluid density (in blue).

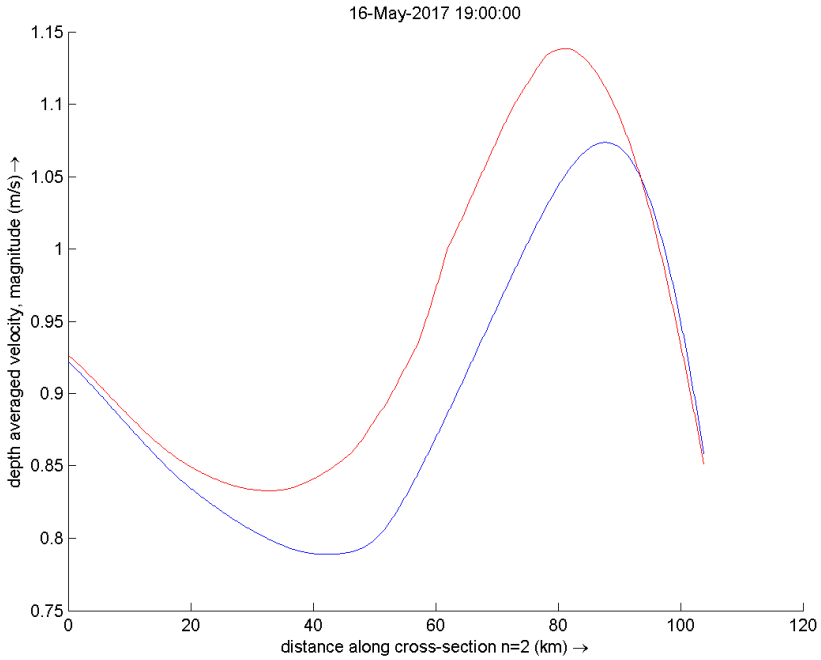

Figure 4.21. Water level over the estuary for simulation 6d (in red), and for the same simulation, but with no effect in fluid density (in blue).

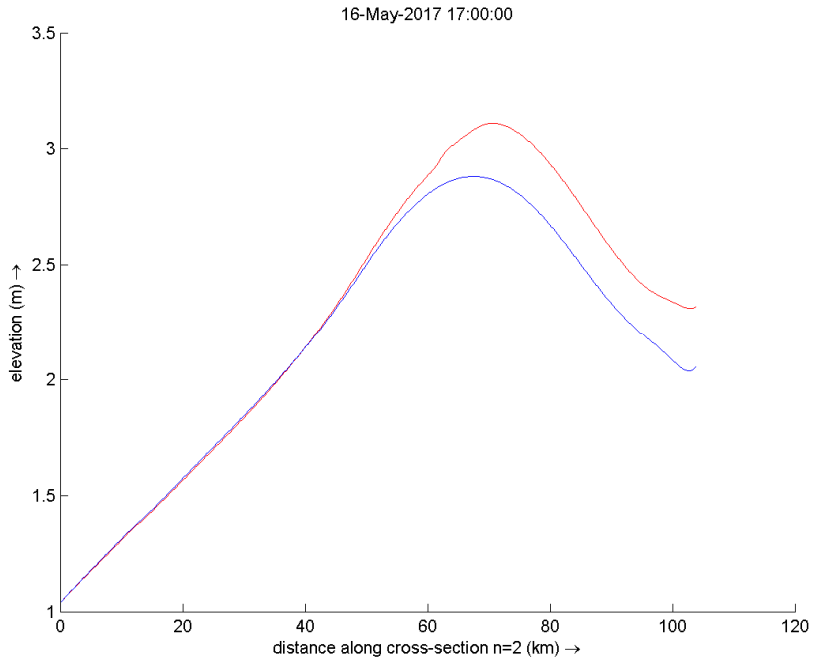

Finally, Figure 4.22 shows the sediment available in the bed for simulation 7a at the end of the simulation period. Note that simulation 7a represents the transition from erosion limited conditions (when hyper-turbidity does not developed because erosion is not enough) to supply limited conditions (when hyper-turbidity does not developed because sediment supply is not enough). Simulation 7a a is supply limited with $\tilde{E}$ = 0.055, but 7f is erosion limited with $\tilde{E}$ = 0.049 (See table 4.1). A increase of $\tilde{E}$ of 0.006 (via the choice of a set of more erosive settings) is behind the transition to supply limited conditions. This means that by increasing the erosion settings the sediment supply stops meeting the demand by erosive processes and the bed becomes empty (or thinner than 5 cm, which is equivalent given the linearly decreased erosion for bed thickness smaller than 5 cm). Figure 4.22 shows indeed a bed where the thickness is always smaller than 5 cm. This would also be the case for any other supply limited simulation discussed in section 4.2: erosion is too large relative the sediment supply, and thus the bed becomes empty (or with a thickness smaller than 5 cm).

Figure 4.22. Sediment in the bed at the end of the simulation period for simulation 7a. Simulation 7a represents the transition from erosion limited to supply limited conditions, as presented in section 4.2.

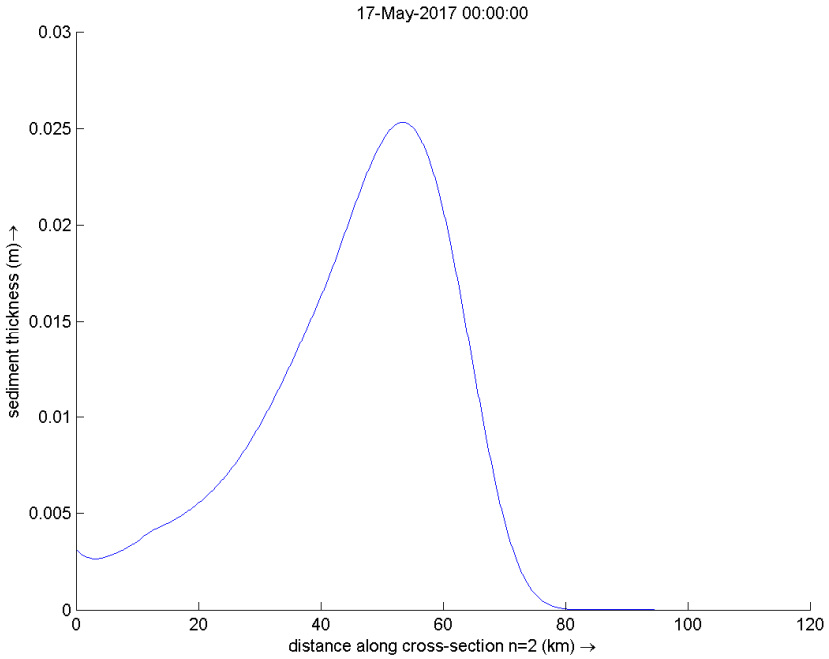

4.4 Evaluating physical considerations of old D3D simulations in iFlow

In order to understand why hyper-turbidity was not achieved over the previous phase of the project, the physical conditions for hyper-turbidity are evaluated for those simulations in appendix A. It was found that neither the sediment erosion parameters (via the dimensionless erosion parameter), nor the sediment availability in the bed (via the erodibility ratio) was fulfilling the conditions for hyper-turbidity. Therefore, it is concluded that those simulations were unsuitable to obtain hyper-turbid conditions in our schematized estuary.

5 Conclusions

This report demonstrated that, in order to achieve and maintain hyper-turbid conditions in a schematized estuary, two conditions need to be fulfilled. The first condition materializes via the parameter $\tilde{E}$, and is fulfilled when $\tilde{E}$ is larger than 0.067. The second condition is 'enough sediment in the bed at the relevant locations throughout the estuary' (i.e. at the locations where sediment can be picked up by the flow without being washed away). This condition materializes via the sediment erodibility parameter, and is fulfilled in D3D when the sediment thickness around the ETM is approximately 1000 times larger than the sediment thickness at the mouth (given realistic SSC at the boundary, or realistic for the Scheldt). This was first formulated theoretically, and later demonstrated via both iFlow (via the erodibility parameter, with different values but similar meaning) and D3D simulation. In fact, the incorporation of these two theoretical considerations resulted in the first D3D simulation showing hyper-turbid conditions since the beginning of the project.

Furthermore, the above mentioned two conditions were assessed for the previous phase of the project. It was concluded that the conditions were indeed not fulfilled for these simulations. . None of the simulations studied in the previous phases had the correct combination of settling and erosion parameters resulting in the adequate value of $\tilde{E}$.
However, when these parameters were modified and the criteria for $\tilde{E}$ were met, hyper-turbidity did still not occur. The latter is because the amount of sediment in the bed over the estuary was very limited in all cases, given the shape and convergence of the estuary and overall its capacity for trapping sediment. This resulted in a 'suboptimal' sediment availability parameter distribution, thereby failing to fulfil one of the two necessary conditions.

Independent from the theoretical formulations and their application to our schematized estuary, this work also provides a study of how varying the parameter space results in different sediment availability ratios and characteristic SSC in D3D. The variations of the parameter space were characterized by the resulting $\tilde{E}$. This analysis was done for a number of model configurations, with the exact same shape and convergence, but with different settling velocities. How the characteristic SSC and the sediment availability ratio changed for varying E is summarized as:

- For estuaries with high trapping capacity (i.e. strong horizontal and vertical convergence and large settling velocity), the estuary's maximum SSC increases linearly with $\tilde{E}$ for small values of $\tilde{E}$, starting to increase exponentially with $\tilde{E}$ once the $\tilde{E}$-threshold of 0.067 is surpassed. Hyper-turbid concentrations develop after this exponential growth.
- For estuaries with high trapping capacity (i.e. strong horizontal and vertical convergence and large settling velocity), the ratio between the sediment availability at the ETM relative to the mouth increases linearly with $\tilde{E}$ for small values of $\tilde{E}$, starting to increase exponentially with $\tilde{E}$ once the $\tilde{E}$ threshold of 0.067 is surpassed. The sediment availability (and erodibility) ratios required for hyper-turbidity develop after this exponential growth.
- For estuaries with a moderate trapping capacity (i.e. strong horizontal and vertical convergence and medium settling velocity), the estuary's maximum SSC increases linearly with $\tilde{E}$ for small values of $\tilde{E}$, but then drops for further increases $\tilde{E}$ due to the transition into supply limited conditions. Supply limited conditions are characterized by a sediment demand from the bed by the erosive processes that cannot be met by the sediment supply to the bed from either outside or elsewhere in the estuary.

- For estuaries with moderate trapping capacity (i.e. strong horizontal and vertical convergence and medium settling velocity), the ratio between the sediment availability at the ETM relative to the mouth increases linearly with $\tilde{E}$ for small values of $\tilde{E}$, but then drops for further increases $\tilde{E}$ due to the transition into supply limited conditions. Supply limited conditions result in an almost empty bed, given the
- For estuaries with small trapping capacity (i.e. strong horizontal and vertical convergence and small settling velocity), the maximum SSC increases when the $\tilde{E}$ threshold is surpassed, but stays several orders of magnitude below from what could be considered as hyper-turbid. The same holds for the sediment availability ratio.

From the detailed analysis of the results from one characteristic hyper-turbid simulation, we can also withdraw a number of conclusions:

- Under constant forcing, and at equilibrium, the bed is empty up until the ETM. The empty region of the bed is supply limited, meaning that demand by erosion dominates supply. Under the ETM, the balance between supply and demand is reverted, supply becomes dominant, and the bed thickness starts building up continuously.
- The sediment flux is constant (after some spin-up time) over the whole estuary until the deposition area, where it becomes zero.
- We can model a hyper-turbid system in D3D where sediment keeps being imported into the system. Under constant forcing, the SSC throughout the estuary arrives to equilibrium once a layer of sediment establishes on the bed under the ETM.
- Sediment induced effects in fluid density play an important role in the development of hyper-turbid conditions in D3D.

Copy for
Marcel Taal, Thijs van Kessel, Bas van Maren, Julia Vroom, Han Winterwerp

Appendix A: Evaluating physical considerations of old D3D simulations in iFlow

In this appendix the conditions for hyper-turbidity discussed in section 0 are checked for the simulations carried out in the previous phase of the project, in order to understand why hyper-turbidity was neither achieved nor maintained in any of these simulations. First, in section A.1, the dimensionless erosion parameter was computed for simulations with the two relevant model configurations in the previous phase, in order to check whether the erosion capacity of the flow and the bed erosion properties were limiting the near-bed concentration. Subsequently, the sediment availability of a number of these simulations was checked in section A.2.

A.1 Dimensionless erosion parameter of previous D3D simulations

Table A.1 shows computed $\tilde{E}$ for the model configuration 3 simulations from the previous phase of the project, as well as for one new simulation with the same model configuration but with different erosive settings. Model configuration 3 was characterized by a standard D3D bed model and no sediment in the bed initially. For this set of simulations, the combinations of the forcing (which is a function of the shape and convergence of the estuary and the tidal motion) and the bed erosive properties led to $\tilde{E} \approx 0.006 - 0.06$. This means that the threshold of $\tilde{E} \approx 0.067$ defined in section 2.1 was not reached. Thus it is not possible to develop high concentrations near the bed and hence hyper-turbid conditions. Therefore we can conclude that either the erosive forces or the erosive settings of the bed were not suitable for the development of hyper-turbid conditions (independently of sediment supply, which may have been insufficient too, and which will be studied later in section 3.2). The maximum concentrations observed in these simulations were indeed 100 to 300 mg/l. In order to achieve hyper-turbidity, concentrations of at least several grams per liter are needed around the turbidity maximum, i.e. hyper-turbid concentrations cannot be obtained with these parameter settings.

In previous report	**3**	**3a**	**3b**	**3d**	**3f[4]-new**
M (kg/m^{2}s)	0.0001	0.001	0.0001	0.001	0.0005
c_{gel} (g/l)	100	100	100	100	100
w_s (m/s)	0.0005	0.0005	0.001	0.001	0.0005
τ_c (Pa)	0.5	0.5	0.5	0.5	0.2
τ_{mean} (Pa)	2	2	2	2	2
$\tilde{E}$ (-)	**0.006**	**0.06**	**0.003**	**0.03**	**0.180**
max SSC (g/l)	0.12	0.16	0.25	0.3	0.12
increase ssc (-)	no	no	no	no	no

Table A.1. $\tilde{E}$ for the simulations with model configuration 3 from the previous phase of the project.

[4] Simulation 3e does exist and is presented in the report from the previous phase, though not presented in this overview.

In order to check if going beyond $\tilde{E} \approx 0.067$ would immediately lead to the development of hyper-turbid conditions, a new simulation was run with the same model configuration, but for different erosive settings. The model settings for this simulation can be found in the rightmost column in table 3.1. In this case, $\tilde{E} > 0.067$, but the SSC did not go beyond 0.2 g/l anywhere in the estuary. This means that though the erosive forces and erosive settings of the bed were correct (condition 1, see section 2), the sediment availability in the bed was most likely not the appropriate (condition 2, see section 2).

Table A.2 shows $\tilde{E}$ computed for simulations with model configuration 5 from the previous phase of the model, as well as for one new simulation with the same model configuration but with different erosive settings. Model configuration 5 was characterized by the inclusion of the buffer layer[5] model for the water-bed exchange rates. Note that $\tilde{E}$ is a function of transfer of mass from the bed to the water column, which changes substantially upon the inclusion of a fluffy layer, as it happens in the buffer layer approach. Therefore, and in order to be able to compute $\tilde{E}$ and study if the forcing was the appropriate for the development of hyper-turbid conditions, the equation of the dimensionless erosion parameter was re-written as follows:

$$\tilde{E} = \left[M_f\left(\tau - \tau_{cr,f}\right) + p_b M_b \left(\frac{\tau - \tau_{cr,b}}{\tau_{cr,b}}\right)^{1.5} \right] \frac{1}{w_{s,0} c_{gel} e_d} \qquad (1.4)$$

$$E_f = M_f\left(\tau_b - \tau_{c,f}\right); \quad M_f = M_{f,0} \times \min\left\{1, m_f / m_{f,c}\right\}$$

where the main differences with equation (1.3) are the inclusion of a deposition efficiency term and the eroded mass coming from both the fluffy layer and the buffer layer (sub-indexes *f* and *b* respectively).

previous report	**5**	**5a**	**5b**	**5c**	**5d**	**5e**	**5g[6]-new**
$M_{f,0}$ (s/m)	0.001	0.001	0.001	0.001	0.001	0.001	0.003
$mf_{,cr}$ (kg)	20	2.5	20	20	20	20	5
c_{gel} (g/l)	50	50	50	50	50	50	50
w_s (m/s)	0.001	0.001	0.001	0.001	0.001	0.001	0.001
e_d (-)	0.2	0.2	0.4	0.2	0.2	0.2	0.2
$\tau_{c,f}$ (Pa)	0.2	0.2	0.2	0.2	0.2	0.2	0.2
τ_{mean} (Pa)	2	2	2	2	2	4	2
p_b (-)	0.09	0.09	0.09	0.3	0.09	0.09	0.09
M_b (kg/m^{2}s)	0.0001	0.0001	0.0001	0.0001	0.0002	0.0001	0.0001
$\tau_{c,b}$ (Pa)	1	1	1	1	0.5	1	1
Approx. m_f	1	0.5	2	2	1	1	1
$\tilde{E}$ (-)	**0.0099**	**0.0369**	**0.0094**	**0.0210**	**0.0458**	**0.0236**	**0.1089**
max SSC (g/)	0.4	0.22	0.25	0.2	0.6	1.1	**1**
increase SSC (-)	mild	no	mild	mild	no	no	**no**

Table A.2 $\tilde{E}$ of the simulations at model configuration 5 from the previous phase of the project, as well as for one new simulation at the same model configuration but with different erosive settings.

[5] For more information on the buffer layer model please see the previous report

[6] Simulation 5f does exist and is presented in the report from the previous phase, though not presented in this overview.

For model configuration 5 simulations, the combinations of the forcing (which is a function of the shape and convergence of the estuary and the tidal motion) and the bed erosive properties led to $\tilde{E} \approx 0.01 - 0.045$. This means that the threshold of $\tilde{E} \approx 0.067$ defined in section 2.1 was not reached. It is thus not possible to develop high concentrations near the bed and hence hyper-turbid conditions. In fact, the largest observed concentration was 1.1 g/l (simulation 5e). This was the equilibrium maximum concentration (i.e. no further increase of SSC over time observed), and not large enough for being considered hyper-turbid. Again, either the erosive forces or the erosive settings of the bed were not the adequate ones.

In order to check if going beyond $\tilde{E} \approx 0.067$ would immediately lead to the development of hyper-turbid conditions, a new simulation was run for the same model configuration, but for different erosive settings. The model settings for this simulation can be found in the rightmost column in table 3.2. In this case, $\tilde{E} > 0.067$, but the SSC did not go beyond 1 g/l anywhere in the estuary. This means that though the erosive forces and erosive settings of the bed were correct (condition 1, see section 2), the sediment availability in the bed was most likely not the appropriate (condition 2, see section 2). In the next section, the sediment availability in the bed throughout the estuary is presented.

A.2 Sediment availability in the bed (erodibility) in former D3D simulations

The sediment availability (proxy for the erodibility concept, see section 2.2) in the simulations from the previous phase of the project was studied via the analysis of the sediment availability in simulation 3 (see table A.1). Simulation 3 is representative for all simulations in the previous phase of the project with respect to sediment availability, since it contains the standard estuary shape and depth, the standard tidal motion, and one of the two standard settling velocities. These are the factors dominating the sediment availability. The sediment availability at simulation 3 was studied by creating an iFlow run that represents simulation 3. Note that an iFlow simulation is needed to be able to directly compute the ratio sediment availability at the mouth to sediment availability at the ETM, as introduced in section 2.2. D3D provides sediment thickness at a specific time step only. Also, note that a direct correlation between iFlow and D3D cannot be established because of the different ways to compute erosion from the bed. In order to obtain erosive settings similar to these in table 3.1, a dimensionless friction height z_0^* of 10^{-4} was set. The rest of the input parameters for this iFlow simulation representing simulation 3 are listed in table A.3. These are exactly the same settings as for simulation 3 (see report from previous phase of the project, as well as table 3.1), with the exception of the already mentioned dimensionless friction height, which represents the erosion settings in iFlow.

Parameter	Description	Value	Unit
H	Depth	6	m
B_0	Width at the mouth	3	km
L_b	Exponential convergence length	30	km
z_0^*	Dimensionless friction height (iFlow model)	$1 \cdot 10^{-4}$	
A_{M_2}	M_2 amplitude at the mouth	2.13	m
A_{M_4}	M_4 amplitude at the mouth	0.14	m
ϕ_{M_2}	M_2 phase at the mouth	91	deg
ϕ_{M_4}	M_4 phase at the mouth	179	deg
Q	River discharge	30	m^3/s
w_s	Fall velocity	$5 \cdot 10^{-4}$	m/s
K_h	Background diffusivity (sediment model)	100	m^2/s

Table A.3. Input parameters iFlow simulation representing simulation 3.

Figure A.1 shows the sediment erodibility over the estuary (with respect to sediment erodibility at the mouth) for the iFlow simulation representing simulation 3. The results show that the erodibility increases in upstream direction over the estuary, but only starting to be significant beyond the 80 km point. Before the 80 km point the erodibility remains very similar to the erodibility at the mouth.

Figure A.1. Sediment erodibility (with respect to erodibility at the mouth) for the iFlow simulation representing simulation 3.

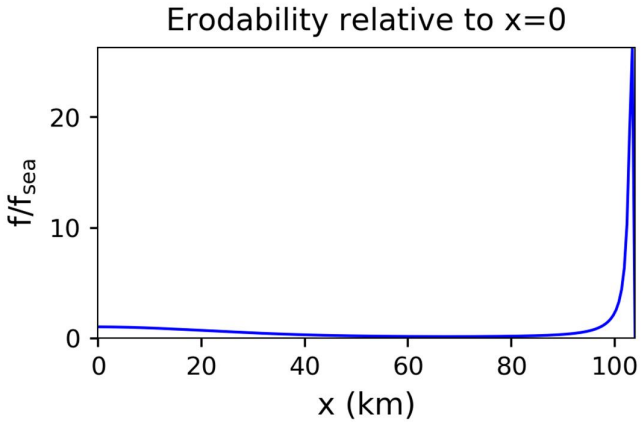

Figure A.2 shows the actual final sediment thickness at the end of simulation 3 in D3D. iFlow predicts accurately the location of the sediment availability peak via the sediment erodibility (at 100 km from the mouth distribution) and the overall sediment erodibility-availability-thickness pattern. We can conclude that the sediment availability is very limited throughout the whole estuary, with the exception of the head of the river. This would hamper the development of hyper-turbid conditions, since enough sediment availability in the bed is a condition for hyper-turbidity as well (condition 2; section 2.2). In fact, this explains why simulations “new” from table 3.1 and table 3.2 did not exhibit high sediment concentration in the water column: the erosive settings and the forcing were the adequate ($\tilde{E}$ > 0.067), but the sediment availability in the bed was not. Again, please note that simulation 3 is representative of simulation 5 type as well, since the settings dominating sediment availability over the estuary (i.e. estuary shape,

depth profile and settling velocity), are the same or very similar. In other words, sediment accumulation takes place at a location where the shear stress is too low to cause resuspension.

Figure A.2. Sediment thickness at the end of the simulation for simulation 3.